VOLUME 111, NUMBER 1
JANUARY 4, 1989

JOURNAL OF THE AMERICAN CHEMICAL SOCIETY

Predictions of Cation Distributions in AB_2O_4 Spinels from Normalized Ion Energies

Robin W. Grimes,[†] Alfred B. Anderson,*[,‡] and Arthur H. Heuer[§]

Contribution from the Department of Chemistry, University of Keele, Keele, Staffs ST5 5BG, U.K., and Department of Chemistry and Department of Materials Science and Engineering, Case Western Reserve University, Cleveland, Ohio 44106. *Received January 11, 1988*

Abstract: A quantum chemical method is developed whereby the structure preference energies for normal- or inverse-structure oxide spinels can be calculated. The method makes use of normalized cation and anion and two-body repulsion energies. Results are given for 50 spinel oxides of known structure, and comparisons are made to the crystal field and classical potential methods.

The spinel structure of AB_2O_4 crystals was first determined in 1915 by Bragg[1] and Nishikawa.[2] The structure is a face-centered cubic arrangement of oxygen ions with metal ions occupying half of the octahedral and one-eighth of the tetrahedral interstitial sites within the anion sublattice (see Figure 1). The way in which the A and B ions are distributed between the two cation sites has long been of interest.

As defined by Barth and Posnjak,[3] if all the tetrahedral sites are occupied by A ions and all the octahedral sites by B ions, $A[B_2]O_4$, the structure is *normal* (the cations inside brackets are in octahedral sites and those outside the brackets are in tetrahedral sites). If the tetrahedral sites are fully occupied by B ions and the octahedral sites are occupied by equal numbers of A and B ions, $B[AB]O_4$, the structure is *inverse*.

The normal and inverse distributions actually represent extreme distributions; a statistical distribution, in which the tetrahedral sites contain $^1/_3$A and $^2/_3$B cations, is referred to as *random*. An inversion parameter, ν,[4] is used in the *mixed* spinel formula:

$$A_{1-\nu}{}^{n+}B_{\nu}{}^{m+}[A_{\nu}{}^{n+}B_{2-\nu}{}^{m+}]O_4{}^{2-}$$

The charge states for A and B cations are $n+$ and $m+$. In fact, many spinel oxides exhibit some degree of mixing in their structure. The degree of disorder will depend on the structure preference energy (SPE) and will of course increase with temperature. Temperature dependence of ν is one experimental measurement of the SPE.[5]

Crystal field theory[6] has often been used to understand cation distributions in spinels. This method defines a set of cation-site preference energies on the basis of the cation coordination and the number of d electrons, which are placed in orbitals whose energies are determined from spectroscopic data. This method is not always successful, and there are unsolved problems when d^0, d^5, and d^{10} ions are present because of a lack of crystal field preference energy.

Structure sorting of spinels has been proposed using a mapping method defined by two quantum mechanical parameters derived from pseudopotential calculations.[7] In this approach, consideration of cation s and p orbitals was claimed to be sufficient and the d orbitals were omitted. This is very different from the crystal field approach, and although predictions agree with experiment in most cases, it is difficult with this type of method to gain insight into the physical reasons associated with structure preference.

Semiempirical approaches to correlating and predicting spinel structures by classical ionic radii and electrostatic interaction energies have been useful.[4,5] The relatively advanced Mott–Littleton potential modeling method has also been applied to the prediction of structure preference for 18 oxide spinels.[8] In each case, the structures were optimized by energy minimization through the METAPOX code. Structure preferences expressed through the difference between calculated crystal energies for normal and inverse distributions were then compared with experiment. Although this method correctly predicted many of the structure preferences, the inclusion of a ligand field preference energy on the basis of the crystal field energies resulted in more correct predictions, including agreement for spinels containing ions that exhibit a strong octahedral site preference such as Cr^{3+}. The drawback with this method is that it does not provide insight into the reasons behind structure preference.

In this paper a normalized ion energy method is applied to 50 spinels of known structure. The theory is found to have good predictive ability, ease of interpretation, and computational simplicity.

[†] Department of Chemistry, University of Keele.
[‡] Department of Chemistry, Case Western Reserve University.
[§] Department of Materials Science and Engineering, Case Western Reserve University.

(1) Bragg, W. H. *Philos. Mag.* **1915**, *30*, 305.
(2) Nishikawa, S. *Proc. Tokyo Math.-Phys. Soc.* **1915**, *8*, 199.
(3) Barth, T. F. W.; Posnjak, E. *J. Wash. Acad. Sci.* **1931**, *21*, 255.
(4) Hill, R. J.; Craig, J. R.; Gibbs, G. V. *Phys. Chem. Miner.* **1979**, *4*, 317.
(5) (a) O'Neill, H. St. C.; Navrotsky, A. *Am. Mineral.* **1983**, *68*, 181. (b) *Ibid.* **1984**, *69*, 733.
(6) (a) Dunitz, J. D.; Orgel, L. E. *J. Phys. Chem. Solids* **1957**, *3*, 318. (b) McClure, D. S. *J. Phys. Chem. Solids* **1957**, *3*, 311.
(7) (a) Burdette, J. K.; Price, G. D.; Price, S. L. *J. Am. Chem. Soc.* **1982**, *104*, 92. (b) *Ibid. Phys. Rev. B* **1981**, *24*, 2903.
(8) (a) Paker, S. C. *Solid State Ionics* **1983**, *8*, 179. (b) Cormack, A. N.; Lewis, G. V.; Parker, S. C.; Catlow, C. R. A. *J. Phys. Chem. Solids*, in press.

0002-7863/89/1511-0001$01.50/0

Table I. Parameters Used in the Calculations[a]

	4s		4p		3d				
atom	IP	ξ	IP	ξ	IP	c_1	ξ_1	c_2	ξ_2
Mg	8.74	1.103	6.04	1.103					
Al	10.42	1.372	5.79	1.356	2.80	0.3000	3.75	0.9000	1.00
Ti	6.32	1.50	4.35	1.20	7.50	0.4206	4.55	0.4839	1.40
V	6.84	1.55	4.81	1.25	8.10	0.4558	4.75	0.7156	1.50
Cr	7.97	1.60	5.84	1.30	9.45	0.4876	4.95	0.7205	1.60
Mn	9.13	1.65	6.85	1.35	10.70	0.5139	5.15	0.6929	1.70
Fe	9.77	1.70	7.34	1.40	10.90	0.5366	5.35	0.6678	1.80
Co	9.96	1.75	7.03	1.45	11.10	0.5551	5.55	0.6461	1.90
Ni	9.54	1.80	6.35	1.50	11.90	0.5683	5.75	0.6292	2.00
Cu	10.63	1.85	6.84	1.55	13.30	0.5819	5.95	0.6120	2.10
Zn	12.19	1.90	8.18	1.60	14.00	0.5951	6.15	0.5951	2.20

	2s		2p	
atom	IP	ξ	IP	ξ
O	26.98	1.946	12.12	1.927

[a] Ionization potentials, IP (eV); Slater orbital exponents, ξ (u); linear coefficients, c. The text explains their origin.

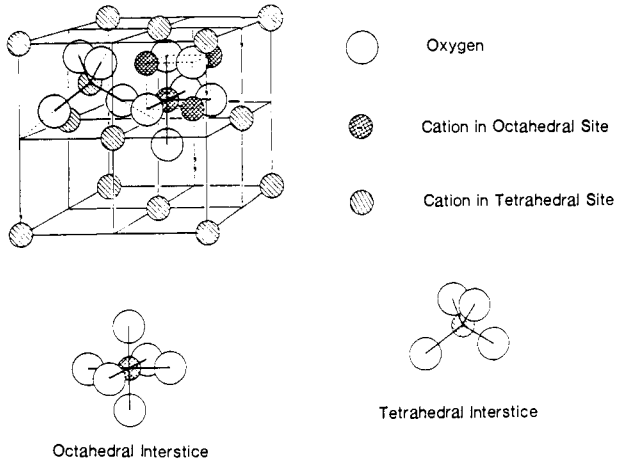

Figure 1. Spinel structure. Oxygen ions are shown in only two octants within the unit cell.

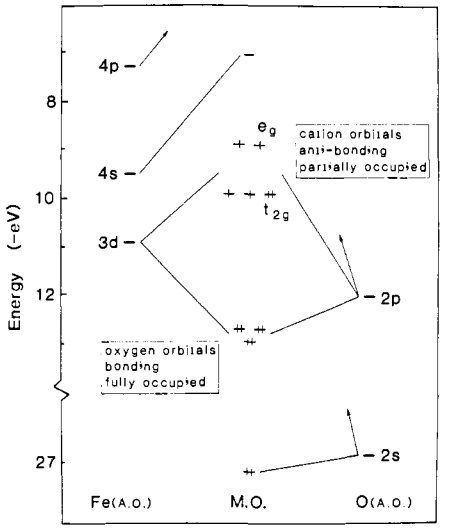

Figure 2. Schematic correlation diagram showing the relationship between the atomic orbitals (AO) and normalized ion molecular orbital (MO) energy levels. This example is for an Fe^{2+} ion in an octahedral environment and O^{2-} in magnetite.

Method

In the normalized ion energy approach the semiempirical ASED-MO theory[9] is used. In this theory the molecular binding energy, E, is partitioned into two components, E_R and E_D (eq 1). For a diatomic molecule E_R is an atom-atom pairwise repulsion energy calculated by integrating the coulombic force on the nucleus of the less electronegative atom caused by the nuclear and atomic charge density of the more electronegative atom. The attractive component, E_D, is calculated by integrating the force on the less electronegative atom's nucleus which is caused by the buildup of bond charge. This is the charge density resulting from the redistribution or delocalization of charge as a bond forms.

$$E = E_R + E_D \quad (1)$$

The atomic density calculated from available valence atomic orbital functions is used for E_R. The bond charge function is not available, so E_D must be estimated. When E_R is determined with the charge density of the more electronegative atom and the nucleus of the other atom, E_D is usually well-approximated as a one-electron molecular orbital interaction energy ΔE_{MO} (eq 2). An extension of this equation to calculate

$$E \simeq E_R + \Delta E_{MO} \quad (2)$$

binding energies of larger molecules and solids requires summing pairwise contributions to E_R.

To obtain the molecular orbital interaction energy, a Hamiltonian similar to extended Hückel is used. The matrix elements, $\mathbf{H}$, are given by eq 3 and 4. The IP's are valence-state ionization potentials (VSIP's)

$$H_{ii} = -IP_i \quad (3)$$

$$H_{ij} = 1.125(H_{ii} + H_{jj}) \exp(-0.13R)S_{ij} \quad (4)$$

taken or deduced from experimental tabulations[10,11] and shifted in value for heteronuclear bonds according to an ionicity constraint; S_{ij} is an overlap integral between orbitals i and j, and R is the internuclear distance. Slater type orbitals are employed, single-ζ type for s and p and double-ζ type for d orbitals. The orbital exponents are taken from SCF atomic wave functions[12,13] and modified according to a diatomic bond length constraint. Valence 4s, 4p, and 3d orbitals are used on the cations and 2s and 2p orbitals on oxygen.

The parameters used in this study for oxygen and the metals Mn through Zn are based on a recent study of diatomic oxides.[14] Values for elements Al, Mg, Ti, V, and Cr are determined specifically for the present work. The parameterization process involves calculating a best fit to the diatomic (MeO) bond length, rather than to charge transfer as was done in ref 14. For the metals Mn through Zn, the two approaches lead to the same parameter values. Parameters used in this paper are given in Table I. For a more complete discussion of the ASED-MO theory, the original theoretical treatment[9] and a more recent discussion[14] may be consulted.

Cluster models and the ASED-MO theory have been used in studies of some bulk oxide properties,[15,16] but the "normalized ion" modeling

(9) (a) Anderson, A. B. *J. Chem. Phys.* **1974**, *60*, 2477. (b) *Ibid.* **1975**, *62*, 1187. The name ASED-MO was applied several years later.

(10) Lotz, W. *J. Opt. Soc. Am.* **1970**, *60*, 206.
(11) Moore, C. E. *Atomic Energy Levels, National Bureau Standards Circular* U.S. Government Printing Office: Washington, DC, 1958; Vol. 467.
(12) Clementi, E.; Raimondi, D. L. *J. Chem. Phys.* **1963**, *38*, 2686.
(13) Richardson, J. W.; Nieuwpoort, W. C.; Powell, R. R.; Edgell, W. F. *J. Chem. Phys.* **1962**, *36*, 1057.
(14) Anderson, A. B.; Grimes, R. W.; Hong, S. Y. *J. Phys. Chem.* **1987**, *91*, 4245.
(15) Debnath, N. C.; Anderson, A. B. *J. Electrochem. Soc.* **1982**, *129*, 2169.

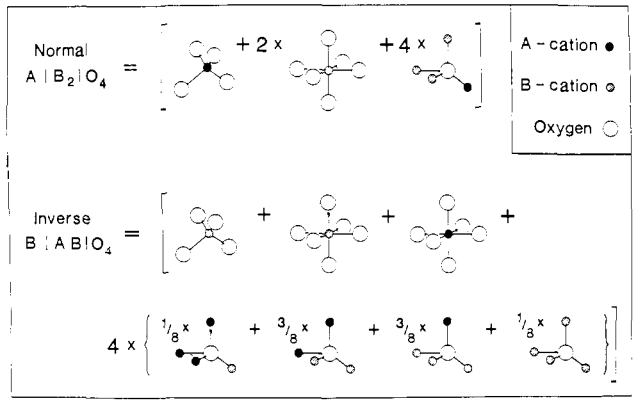

Figure 3. Normalized ion clusters that provide the nearest-neighbor crystal environment around constituent ions of formula units for both normal and inverse spinel structures.

approach was developed to predict the most stable defect structures in the monoxides MnO, FeO, CoO, and NiO.[17-19] The extension to spinels is straightforward. In essence, the normalized ion energies (NIE) are valence electron energies for cations and anions in the rigid anion sublattice. They are calculated with "local coordination" clusters and for a particular anion or cation are given by the formula

$$\mathrm{NIE} = \sum_i n_i e_i \tag{5}$$

where e_i is the energy of orbital i and n_i is its occupation (0–2). For oxides the cation NIE is calculated by summing over the metal–oxygen antibonding counterpart orbitals, and for the anion NIE the sum is over the doubly occupied O 2s and 2p orbitals; as discussed below, Zn^{2+} is an exception. A typical example of the electronic structure is shown in Figure 2. A high-spin cation occupation is assumed throughout, as indicated in ref 4.

Local coordinations in the spinel structure are shown in Figure 3. For a normal spinel the total normalized ion energy is

$$\mathrm{NIE^T(n) = NIE^A(t) + 2NIE^B(o) + 4NIE^O(n)} \tag{6}$$

where T stands for total and n, t, and o stand for normal, tetrahedral, and octahedral, respectively. The formula is given visually in Figure 3. The total normalized ions energy for an inverse spinel is

$$\mathrm{NIE^T(i) = NIE^B(t) + NIE^A(o) + NIE^B(o) + 4NIE^O(i)} \tag{7}$$

When there is no cation ordering in the octahedral sites (assumed throughout), $\mathrm{NIE^O(i)}$ has four components (eq 8). This is also shown visually in Figure 3.

$$\mathrm{NIE^O(i) = NIE^O(o_{AAA}t_B)/8 + 3NIE^O(o_{BAA}t_B)/8 + 3NIE^O(o_{BBA}t_B)/8 + NIE^O(o_{BBB}t_B)/8} \tag{8}$$

The total two-body repulsive energy of the ASED–MO theory, E_R, is added to the total normalized ion energies to yield the total energy. For a normal spinel

$$E_R^T(n) = 4E_R(\mathrm{A\text{–}O})(t) + 12E_R(\mathrm{B\text{–}O})(o) \tag{9}$$

Here, the 4 two-body energies for the tetrahedrally coordinated A cation and 12 for the two octahedrally coordinated B cations are summed. For the inverse spinel

$$E_R^T(i) = 4E_R(\mathrm{B\text{–}O})(t) + 6E_R(\mathrm{B\text{–}O})(o) + 6E_R(\mathrm{A\text{–}O})(o) \tag{10}$$

The energy of a normal spinel is then

$$E(n) = \mathrm{NIE^T}(n) + E_R^T(n) \tag{11}$$

and for an inverse spinel

$$E(i) = \mathrm{NIE^T}(i) + E_R^T(i) \tag{12}$$

The structure preference energy is eq 12 – eq 11.

$$\mathrm{SPE} = E(i) - E(n) \tag{13}$$

Because detailed crystallographic data generally are found for only one spinel cation arrangement and because of the enormous simplification to the theoretical calculations, a single average lattice parameter of 8.40 Å has been chosen for all spinel structures (the experimental lattice parameters for compounds studied here all lie between 8.10 and 8.60 Å). The lattice is assumed to have perfect symmetry; that is, the u parameter is 0.375.

Results and Discussion

Total structure energies and structure preference energies are presented in Table II. For the aluminates, chromites, ferrites, manganites, and vanadates, there is a common majority cation. Results for some miscellaneous spinels follow the vanadate results.

A positive SPE means the normal cation distribution is predicted to be more stable, and a negative value means the inverse distribution is preferred. A mixed structure is indicated as M–I or M–N, depending on whether its ν parameter is greater than or less than $^2/_3$. When a structure is mixed, it is clear that the SPE is relatively small compared to kT in the temperature range of appreciable cation mobility. The results given below indicate that the predicted site preference energies should be viewed qualitatively for determining structure type and not quantitatively for predicting ν in mixed spinels. In order to develop a physical understanding of why one cation arrangement is more stable than another, one can examine the components of the electronic contribution to the structure preference energy.

Anion Preference Energy. This energy is the oxygen normalized ion energy in the inverse structure minus that for the normal structure. The extent of the bonding stabilization depends on the properties of the surrounding cations. When the A cation stabilizes the oxygen orbitals more than the B cation, the oxygen preference energy will favor the normal structure, with A cations in tetrahedral sites where the AO bond is shorter. Otherwise, the oxygen preference energy favors the inverse structure.

The oxygen orbital stabilization increases with metal–oxygen orbital overlap and decreases with the difference in metal and oxygen energy levels. For the case of metal d and O 2p interactions this is seen in the expression from second-order perturbation theory (eq 14) where ΔE is the stabilization, H′ is the interaction

$$\Delta E = |(\Psi_d|H'|\Psi_p\rangle|^2/(e_d - e_p) \tag{14}$$

Hamiltonian, and Ψ and e are orbital wave functions and energies. Since the oxygen orbital energy levels are fixed in this work, the variations in metal orbital energy levels are important. Also important is the larger d–p overlap and hence larger numerator for tetrahedral metal coordination than for octahedral coordination, a consequence of shorter tetrahedral bond lengths.

Equation 14 is applied to understanding structures of the chromites as follows. Valence orbital energy levels for Mg^{2+}, Al^{3+}, Ti^{4+}, and V^{3+} lie above Cr^{3+}, and those for Mn^{2+}, Fe^{2+}, Co^{2+}, Ni^{2+}, and Cu^{2+} lie below. Therefore, the normalized oxygen energy favors the first set of cations taking octahedral positions (inverse structure) and the second set of cations taking the tetrahedral positions (normal structure). Figure 4 shows the corresponding anion preference energies for chromites as well as the aluminates,

(16) Anderson, A. B. *Chem. Phys. Lett.* **1980**, *72*, 514.
(17) Grimes, R. W.; Anderson, A. B.; Heuer, A. H. *J. Phys. Chem. Solids* **1987**, *48*, 45.
(18) Grimes, R. W.; Anderson, A. B.; Heuer, A. H. *J. Am. Ceram. Soc.* **1986**, *69*, 619.
(19) Anderson, A. B.; Grimes, R. W.; Heuer, A. H. *J. Solid State Chem.* **1984**, *55*, 353.
(20) Grimes, N. W.; Thompson, P.; Kay, H. F. *Proc. R. Soc. London A* **1983**, *386*, 333.
(21) Layden, G. K. *J. Am. Ceram. Soc.* **1965**, *48*, 219.
(22) Verwey, E. J.; Heilmann, E. L. *J. Chem. Phys.* **1947**, *15*, 174.
(23) Ishikawa, Y.; Sato, S.; Syono, Y. *J. Phys. Soc. Jpn.* **1971**, *31*, 452.
(24) Levinstein, H. J.; Robbins, M.; Capio, C. *Mater. Res. Bull.* **1972**, *7*, 27.
(25) Rieck, G. D.; Driessens, F. C. M. *Acta Crystallogr.* **1966**, *20*, 521.
(26) Shull, C. G.; Wollan, E. O.; Koehler, W. C. *Phys. Rev.* **1951**, *84*, 912.
(27) Rhadakrishnam, N. K.; Biswas, A. B. *Phys. Status Solidi A* **1968**, *37*, 719.
(28) Buhl, R. *J. Phys. Chem. Solids* **1969**, *30*, 805.
(29) Boucher, B.; Buhl, R.; Perrin, M. *J. Appl. Phys.* **1968**, *39*, 632.
(30) Ishii, I.; Nakamura, T. *Rep. Res. Lab. Eng. Mater., Tokyo Inst. Technol.* **1981**, *6*, 63.
(31) de Graef, M.; Seinen, P. A.; Ijdo, D. J. W. *J. Sol. State Chem.* **1985**, *58*, 357.

Table II. Results for Spinels[a]

spinel	type[b]	cation distribution (tet, oct, oct)	total structure energy	anion preference energy	cation preference energy		structure preference energy		METAPOCS[d]
					av	splitting	ASED	C-F[c]	
			Aluminates (AAl_2O_4)						
$MgAl_2O_4$	N[20]	$Mg^{2+}Al^{3+}Al^{3+}$	-526.594	1.02	0.00	0.00	1.06	0.00	0.86
		$Al^{3+}Mg^{2+}Al^{3+}$	-525.537						
$MnAl_2O_4$	N	$Mn^{2+}Al^{3+}Al^{3+}$	-578.316	4.06	-0.12	0.00	3.73	0.00	1.83
		$Al^{3+}Mn^{2+}Al^{3+}$	-574.589						
$FeAl_2O_4$	N	$Fe^{2+}Al^{3+}Al^{3+}$	-590.965	4.11	-0.82	-0.74	2.06	-0.17	1.09
		$Al^{3+}Fe^{2+}Al^{3+}$	-588.903						
$CoAl_2O_4$	N	$Co^{2+}Al^{3+}Al^{3+}$	-602.486	3.82	-1.84	-1.00	0.46	-0.32	0.75
		$Al^{3+}Co^{2+}Al^{3+}$	-602.028						
$NiAl_2O_4$	I	$Ni^{2+}Al^{3+}Al^{3+}$	-618.105	4.23	-3.30	-1.79	-1.43	-0.89	0.11
		$Al^{3+}Ni^{2+}Al^{3+}$	-619.534						
$CuAl_2O_4$	M-N (ν = 0.4)	$Cu^{2+}Al^{3+}Al^{3+}$	-648.921	6.54	-4.13	-0.65	1.15	-0.35	
		$Al^{3+}Cu^{2+}Al^{3+}$	-647.772						
$ZnAl_2O_4$	N	$Zn^{2+}Al^{3+}Al^{3+}$	-682.214	-0.04	2.45	0.00	1.76	0.00	1.73
		$Al^{3+}Zn^{2+}Al^{3+}$	-680.450						
			Chromites (ACr_2O_4)						
$MgCr_2O_4$	N	$Mg^{2+}Cr^{3+}Cr^{3+}$	-575.616	-1.84	-1.19	4.86	2.28	1.63	1.47
		$Cr^{3+}Mg^{2+}Cr^{3+}$	-573.337						
Cr_3O_4	N[21]	$Cr^{2+}Cr^{3+}Cr^{3+}$	-608.002	0.00	-0.41	2.43	2.84	0.89	
		$Cr^{3+}Cr^{2+}Cr^{3+}$	-605.165						
$MnCr_2O_4$	N	$Mn^{2+}Cr^{3+}Cr^{3+}$	-625.611	1.55	-1.08	4.87	5.30	1.63	2.27
		$Cr^{3+}Mn^{2+}Cr^{3+}$	-620.310						
$FeCr_2O_4$	N	$Fe^{2+}Cr^{3+}Cr^{3+}$	-638.243	1.67	-1.99	4.09	3.70	1.46	1.66
		$Cr^{3+}Fe^{2+}Cr^{3+}$	-634.542						
$CoCr_2O_4$	N	$Co^{2+}Cr^{3+}Cr^{3+}$	-649.980	1.43	-3.03	3.86	2.15	1.31	1.35
		$Cr^{3+}Co^{2+}Cr^{3+}$	-647.831						
$NiCr_2O_4$	N	$Ni^{2+}Cr^{3+}Cr^{3+}$	-665.768	2.18	-4.50	3.08	0.61	0.74	0.56
		$Cr^{3+}Ni^{2+}Cr^{3+}$	-665.163						
$CuCr_2O_4$	N	$Cu^{2+}Cr^{3+}Cr^{3+}$	-696.397	5.26	-5.34	4.22	3.94	1.28	
		$Cr^{3+}Cu^{2+}Cr^{3+}$	-692.454						
$ZnCr_2O_4$	N	$Zn^{2+}Cr^{3+}Cr^{3+}$	-730.680	-2.04	1.29	4.82	3.84	1.63	2.33
		$Cr^{3+}Zn^{2+}Cr^{3+}$	-726.838						
			Ferrites (AFe_2O_4)						
$MgFe_2O_4$	M-I (ν = 0.9)	$Mg^{2+}Fe^{3+}Fe^{3+}$	-622.391	-2.91	0.70	0.00	-1.68	0.00	-0.67
		$Fe^{3+}Mg^{2+}Fe^{3+}$	-624.074						
$AlFe_2O_4$	I[22]	$Al^{3+}Fe^{3+}Fe^{2+}$	-636.030	-3.68	0.70	0.00	-2.49	0.00	-0.23
		$Fe^{3+}Al^{3+}Fe^{2+}$	-638.521						
$TiFe_2O_4$	I[23]	$Ti^{4+}Fe^{2+}Fe^{2+}$	-642.661	-3.43	0.84	0.72	-1.72	0.17	-0.20
		$Fe^{2+}Ti^{4+}Fe^{2+}$	-644.381						
VFe_2O_4	I	$V^{3+}Fe^{3+}Fe^{2+}$	-645.223	-2.81	2.57	-3.78	-3.91	-0.53	
		$Fe^{3+}V^{3+}Fe^{2+}$	-649.135						
$CrFe_2O_4$	I[24]	$Cr^{3+}Fe^{3+}Fe^{2+}$	-657.310	-1.48	1.88	-4.85	-4.37	-1.63	-1.03
		$Fe^{3+}Cr^{3+}Fe^{2+}$	-661.687						
$MnFe_2O_4$	M-N[25] (ν = 0.2)	$Mn^{2+}Fe^{3+}Fe^{3+}$	-670.529	-0.16	0.82	0.00	0.69	0.00	0.21
		$Fe^{3+}Mn^{2+}Fe^{3+}$	-669.835						
Fe_3O_4	I[26]	$Fe^{2+}Fe^{3+}Fe^{3+}$	-683.043	0.00	-0.14	-0.72	-0.86	-0.17	-0.51
		$Fe^{3+}Fe^{2+}Fe^{3+}$	-683.899						
$CoFe_2O_4$	I	$Co^{2+}Fe^{3+}Fe^{3+}$	-694.919	-0.18	-1.14	-1.00	-2.35	-0.32	-0.82
		$Fe^{3+}Co^{2+}Fe^{3+}$	-697.273						
$NiFe_2O_4$	I	$Ni^{2+}Fe^{3+}Fe^{3+}$	-710.177	0.24	-2.67	-1.77	-4.23	-0.89	-1.63
		$Fe^{3+}Ni^{2+}Fe^{3+}$	-714.403						
$CuFe_2O_4$	I	$Cu^{2+}Fe^{3+}Fe^{3+}$	-737.687	3.06	-3.44	-0.65	-1.14	-0.35	
		$Fe^{3+}Cu^{2+}Fe^{3+}$	-738.828						
$ZnFe_2O_4$	N	$Zn^{2+}Fe^{3+}Fe^{3+}$	-775.186	-2.23	3.14	0.00	0.77	0.00	0.20
		$Fe^{3+}Zn^{2+}Fe^{3+}$	-774.417						
			Manganites (AMn_2O_4)						
$MgMn_2O_4$	M-N[27] (ν = 0.22)	$Mg^{2+}Mn^{3+}Mn^{3+}$	-602.169	-2.87	-0.09	1.88	-0.60	-0.45	
		$Mn^{3+}Mg^{2+}Mn^{3+}$	-602.767						
$TiMn_2O_4$	I	$Ti^{4+}Mn^{2+}Mn^{2+}$	-614.065	-3.42	-0.12	0.00	-3.42	0.00	
		$Mn^{2+}Ti^{4+}Mn^{2+}$	-617.489						
VMn_2O_4	M-I (ν = 0.8)	$V^{3+}Mn^{2+}Mn^{3+}$	-621.075	-2.78	1.77	-3.80	-4.44	-1.53	
		$Mn^{2+}V^{3+}Mn^{3+}$	-625.519						
		$V^{4+}Mn^{2+}Mn^{2+}$	-621.007	-2.78	0.84	-1.90	-3.49		
		$Mn^{2+}V^{4+}Mn^{2+}$	-624.492						
$CrMn^2O_4$	I[27]	$Cr^{3+}Mn^{2+}Mn^{3+}$	-633.028	-1.39	-1.09	-4.88	-5.14	-1.63	
		$Mn^{2+}Cr^{3+}Mn^{3+}$	-638.168						
Mn_3O_4	N	$Mn^{2+}Mn^{3+}Mn^{3+}$	-650.483	0.00	0.03	1.88	1.91	0.45	
		$Mn^{3+}Mn^{2+}Mn^{3+}$	-648.577						
$FeMn_2O_4$	M-I[18] (ν = 0.91)	$Fe^{3+}Mn^{2+}Mn^{3+}$	-659.819	0.16	-0.82	0.00	-0.70	0.00	
		$Mn^{2+}Fe^{3+}Mn^{3+}$	-660.516						
$CoMn_2O_4$	M-N[29] (ν = 0.22)	$Co^{2+}Mn^{3+}Mn^{3+}$	-674.882	-0.04	-1.93	0.88	-1.16	0.13	
		$Mn^{3+}Co^{2+}Mn^{3+}$	-676.045						
		$Co^{2+}Mn^{2+}Mn^{4+}$	-674.882	-0.04	-1.92	-1.00	-3.07	-0.32	
		$Mn^{2+}Co^{2+}Mn^{4+}$	-677.952						

Table II (Continued)

spinel	type[b]	cation distribution (tet, oct, oct)	total structure energy	anion preference energy	cation preference energy		structure preference energy		METAPOCS[d]
					av	splitting	ASED	C-F[c]	
$NiMn_2O_4$	M-I (ν = 0.93)	$Ni^{2+}Mn^{3+}Mn^{3+}$	-690.169	0.44	-3.39	0.09	-2.98	-0.44	
		$Mn^{3+}Ni^{2+}Mn^{3+}$	-693.148						
		$Ni^{2+}Mn^{2+}Mn^{4+}$	-690.169	0.44	-3.46	-1.77	-4.89	-0.89	
		$Mn^{2+}Ni^{2+}Mn^{4+}$	-695.054						
$CuMn_2O_4$	M-N[28] (ν = 0.24)	$Cu^{2+}Mn^{3+}Mn^{3+}$	-718.122	3.48	-4.23	1.23	0.32	0.10	
		$Mn^{3+}Cu^{2+}Mn^{3+}$	-717.797						
		$Cu^{1+}Mn^{3+}Mn^{4+}$	-722.528	3.48	-4.68	1.88	0.56	0.99	
		$Mn^{3+}Cu^{1+}Mn^{4+}$	-721.971						
$ZnMn_2O_4$	N[28]	$Zn^{2+}Mn^{3+}Mn^{3+}$	-755.294	-2.35	2.35	1.88	1.69	0.45	
		$Mn^{3+}Zn^{2+}Mn^{3+}$	-753.602						
			Vanadates (AV_2O_4)						
MgV_2O_4	N	$Mg^{2+}V^{3+}V^{3+}$	-548.073	-0.63	-1.88	3.80	1.69	0.53	
		$V^{3+}Mg^{2+}V^{3+}$	-546.376						
AlV_2O_4	N[30]	$Al^{3+}V^{3+}V^{2+}$	-558.222	-1.76	-1.88	3.80	0.54	0.53	
		$V^{3+}Al^{3+}V^{2+}$	-557.684						
MnV_2O_4	N	$Mn^{2+}V^{3+}V^{3+}$	-598.674	3.20	-1.78	3.81	4.28	0.53	
		$V^{3+}Mn^{2+}V^{3+}$	-594.393						
FeV_2O_4	N	$Fe^{2+}V^{3+}V^{3+}$	-612.251	3.26	-2.70	3.06	3.51	0.36	
		$V^{3+}Fe^{2+}V^{3+}$	-608.742						
CoV_2O_4	N	$Co^{2+}V^{3+}V^{3+}$	-623.857	3.00	-3.72	2.80	1.93	0.21	
		$V^{3+}Co^{2+}V^{3+}$	-621.932						
ZnV_2O_4	N	$Zn^{2+}V^{3+}V^{3+}$	-704.632	-1.43	0.60	3.76	2.67	0.53	
		$V^{3+}Zn^{2+}V^{3+}$	-701.966						
			Miscellaneous						
$TiCo_2O_4$	I	$Ti^{4+}Co^{2+}Co^{2+}$	-669.221	-3.11	1.84	1.00	-0.08	0.32	
		$Co^{2+}Ti^{4+}Co^{2+}$	-660.300						
VCo_2O_4	I	$V^{4+}Co^{2+}Co^{2+}$	-675.829	-2.52	2.77	-0.89	-0.48		
		$Co^{2+}V^{4+}Co^{2+}$	-676.313						
$MnTi_2O_4$	N	$Mn^{2+}Ti^{3+}Ti^{3+}$	-583.236	3.87	-1.57	2.74	4.92	0.33	
		$Ti^{3+}Mn^{2+}Ti^{3+}$	-578.316						
$MgTi_2O_4$	N	$Mg^{2+}Ti^{3+}Ti^{3+}$	-531.283	0.12	-1.69	2.74	1.30	0.33	
		$Ti^{3+}Mg^{2+}Ti^{3+}$	-529.979						
$TiZn_2O_4$	I	$Ti^{4+}Zn^{2+}Zn^{2+}$	-824.371	-0.39	-2.44	0.00	-2.53	0.00	
		$Zn^{2+}Ti^{4+}Zn^{2+}$	-826.898						
VZn_2O_4	I	$V^{4+}Zn^{2+}Zn^{2+}$	-830.453	-0.20	-1.51	-1.89	-3.34		
		$Zn^{2+}V^{4+}Zn^{2+}$	-833.793						
$TiNi_2O_4$	N(?)[31]	$Ti^{4+}Ni^{2+}Ni^{2+}$	-703.785	-3.44	3.31	1.78	1.88	0.89	
		$Ni^{2+}Ti^{4+}Ni^{2+}$	-701.904						
$TiMg_2O_4$	I	$Ti^{4+}Mg^{2+}Mg^{2+}$	-518.421	0.11	0.00	0.00	-0.26	0.00	
		$Mg^{2+}Ti^{4+}Mg^{2+}$	-518.681						

[a] Energies in electronvolts. Positive structure preference energies mean the normal structure is more stable than inverse. Comparisons of ASED-calculated total structural energies and their components with data from other models. The two-body structure preference energy can be obtained by substracting the anion and cation preference energies from the structure preference energy. [b] All experimental structural data unless otherwise stated are from ref 4. N = normal, I = inverse, M-I = mixed inverse, $\nu > {}^2/_3$, M-N = mixed normal, $\nu < {}^2/_3$. [c] Crystal field results from Dunitz and Orgel.[6] [d] METAPOCS is the classical potential modeling code employed in ref 8.

vanadates, and ferrites. Anion preference energies for the latter three parallel those for the chromites across the series for the same reasons. The Zn^{2+} 3d levels lie below the O 2p levels so that the 2p levels are destabilized. Since this destabilization is less for octahedral coordination, the anion preference energy favors the inverse structure in $B[ZnB]O_4$ spinels.

Cation Preference Energy. With the exception of Zn^{2+}, the metal 3d energy levels lie above the O 2p levels. Therefore, for all but Zn^{2+}, the d splittings are as in Figure 5, with the average tetrahedral shift greater than the average octahedral shift because of the shorter tetrahedral bond distances. It is noted that the crystal field approach to predicting spinel structures is based on occupying octahedrally and tetrahedrally split energy levels as in Figure 5 but with the same average value for all cations. In the present work, the cation contribution to the structure preference energy include both the average d and splitting energy differences; they are given in Table II. The total structure preference energy is the sum of this and the anion and two-body repulsion structure preference energies. Crystal field predictions use only the splitting structure preference energies, with the splittings taken from optical excitation spectra. Some structure preference energies based on average d orbital energies may be seen in Figure 6, and calculated octahedral site preference energies for a series of cations are in Figure 7; the experimental results shown in Figure 7 will be discussed below, but, first, five spinels are analyzed.

1. Fe_3O_4 (Magnetite). The two possible cation arrangements are $Fe^{2+}[Fe_2^{3+}]O_4$ and $Fe^{3+}[Fe^{2+}Fe^{3+}]O_4$. Since there is no change in atomic species between the distributions, the anion preference energy is zero, and since the change from normal to inverse structure involves only the exchange of one electron, the average d orbital preference energy is small. Therefore, the crystal-field-like splitting energy dominates the structure preference energy and makes this structure inverse.

2. $MgAl_2O_4$ (Spinel). Neither Mg or Al have any d orbital occupation, so the cation d electron site preference energy is zero. The observed normal cation arrangement is therefore entirely due to the anion preference energy.

3. $CrFe_2O_4$ (Chromium Ferrite). The Cr^{3+} ion is d^3, and therefore it has a very strong octahedral site preference energy. This dominates the cation contribution, and because the anion and average d contributions are of the same order of magnitude and opposite sign, they nearly cancel. The d orbital crystal-field-like splitting energy can be said to cause the formation of the inverse structure.

4. $MnFe_2O_4$ (Jacobsite). Both Mn^{2+} and Fe^{3+} are d^5 ions and therefore have a zero d-orbital splitting site preference energy. Since Mn and Fe are next to each other in the periodic table and

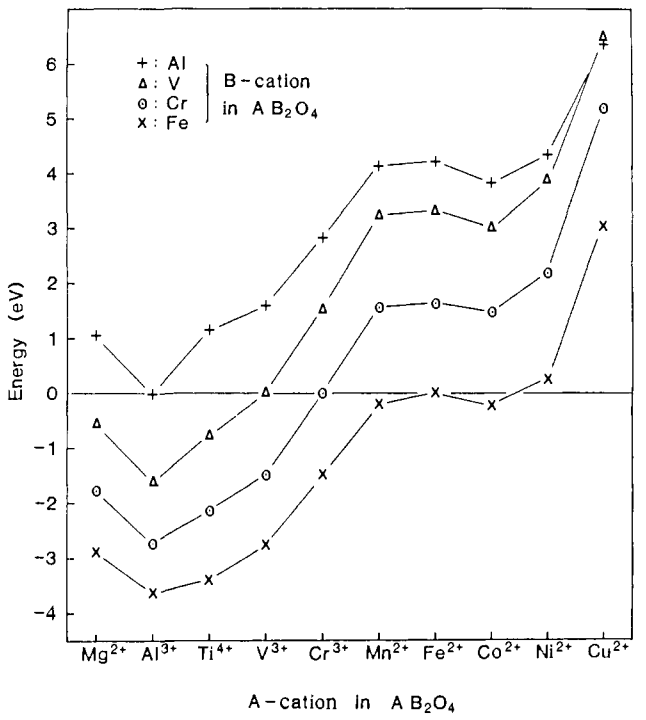

Figure 4. Anion preference energies as ordered by atomic number. Positive values favor the normal spinel structure and negative values the inverse structure.

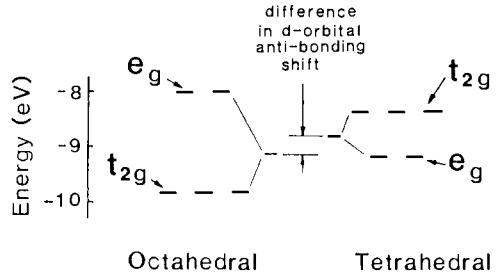

Figure 5. Pictorial representation of the cation site preference energies based on average d orbital energies.

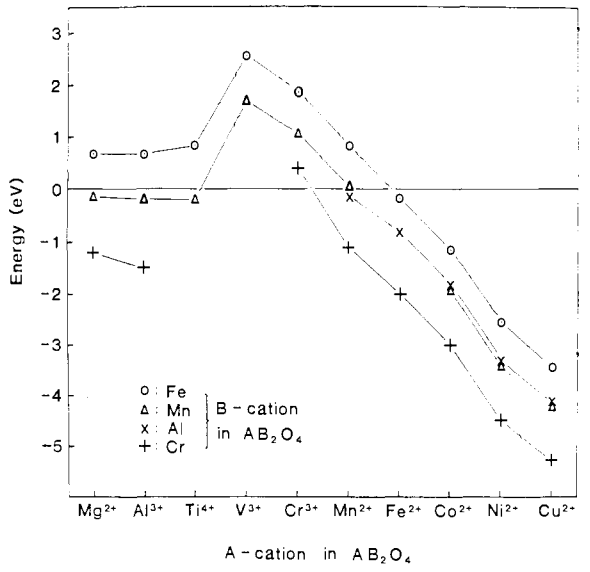

Figure 6. Structure preference energies based on average d orbital energies for a selected series of compounds. Positive values favor the normal spinel structure and negative values the inverse structure.

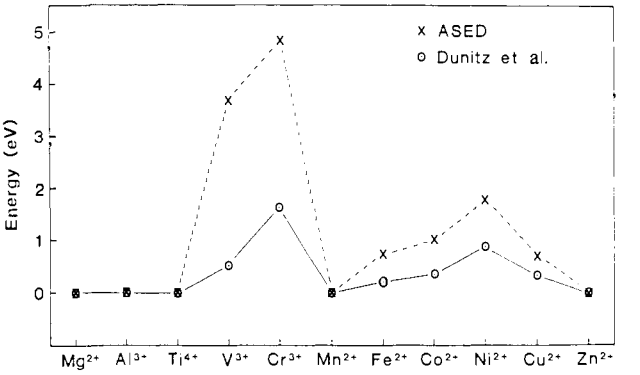

Figure 7. Crystal-field-like octahedral site preference energies for metal ions as calculated from metal 3d orbital splittings. Dunitz results from ref 6a supplemented by ref 6b.

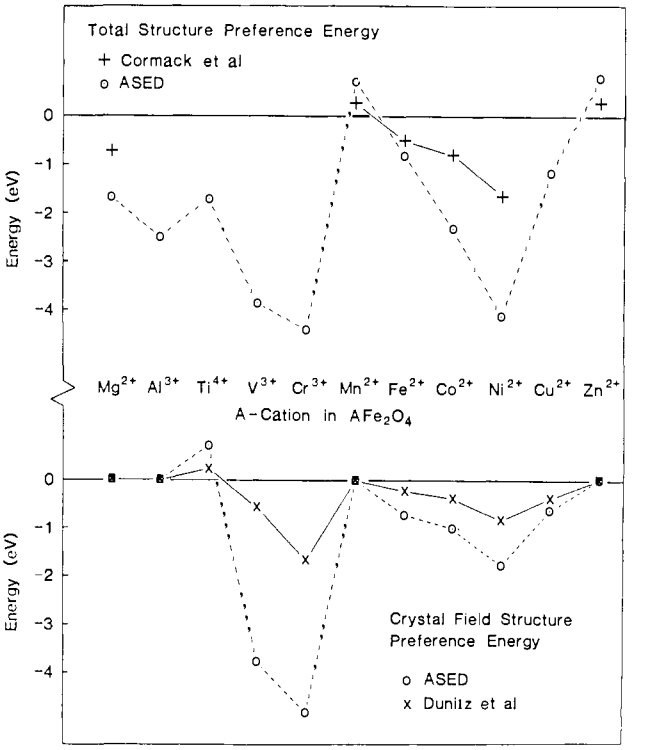

Figure 8. Comparison of cation structure preference energies obtained by various methods for the ferrites (AFe_2O_4). Cormack results from ref 8b; Dunitz results from ref 6a supplemented by ref 6b.

have similar orbital sizes and energy levels, their oxygen orbital stabilizations are similar, leading to a small anion preference energy. This periodic relationship also causes the average d cation preference to be small, resulting in $MnFe_2O_4$ having a small cation distribution preference. The small net normal structure preference energy agrees with the randomness of the observed structure with $\nu = 0.2$.

5. $TiFe_2O_4$ (Ulvöspinel). In this last example, the two dissimilar cations give rise to a significant anion structure preference energy. Because Fe stabilizes the oxygen orbitals much more than Ti, there is a strong preference for Fe to occupy the tetrahedral site and therefore form the inverse structure seen experimentally. While the Fe^{2+} ion causes the d orbital splitting preference energy to be positive, favoring a normal distribution, this is swamped by the anion preference energy. The average d preference energy also favors the normal structure, but the relatively small number of electrons involved makes this contribution small. In this example the present method correctly predicts an inverse cation distribution because of the inclusion of the anion preference energy; the crystal-field-like energy difference is insufficient and the crystal field approach fails.

There are two cases where the normalized ion ASED-MO approach disagrees with experiment, $MgMn_2O_4$ and $CoMn_2O_4$, both of which are mixed normal. However, the manganite family is extremely variable experimentally in its SPE. The crystal field approach also has trouble with these compounds.

Generally, the anion preference energy is important for compounds where the two cations have very different atomic numbers. It is least important for adjacent members of the periodic table. Cation preference energies are less simply characterized, being subject to both average d shift and splitting effects.

The d splitting site preference energies based on ASED-MO calculations are analogous to the empirically determined crystal field site preference energies of Dunitz and Orgel.[6a] A comparison of the two, given in Figure 7, shows the ASED-MO crystal field octahedral site preference energies overestimate the empirical values. The ASED-MO crystal field structure preference energies also overestimate the empirical ones, in a similar way, as shown in the case of the ferrites in the lower part of Figure 8. The other site preference energy components are required in order to make correct structure predictions in the cases of the Mg, Al, Mn, and Zn ferrites, as shown in the upper part of Figure 8. Comparison of the total structure preference energies with those of the Mott-Littleton potential modeling technique[7a,b] shows agreement in sign, but the ASED-MO values are larger by a factor of about 2. It is significant that the two approaches yield the same trend. The ASED-MO normalized ion approach details the physical reasons in terms of electronic structure. It is interesting that the two-body energy contributions to the structure preference energies, which can be determined from the data in Table II by subtracting the anion and cation preference energies from the structure preference energies, are small, and in only one case, $TiMg_2O_4$, does this energy determine the structure preference.

Conclusion

Predictions for the site preference energies of oxide spinels have been made for 50 compounds. The consideration of the ASED-MO cation and anion orbital energy levels reveals why a particular cation distribution is dominant over another. This is an improvement over the crystal field approach, which considers only the cation energies in an approximate way. The theoretical cation structure preference energy has been partitioned into two portions so that the crystal-field-like terms can be separately evaluated. The theoretical crystal field component is just as good (or bad) as crystal field theory for predicting whether an oxide spinel is normal or inverse. The two-body repulsion site preference energy is responsible for the structure in only one of the 50 compounds. The anion and two-body repulsion site preference energies provide the necessary corrections to the crystal field energies.

Acknowledgment. The initial stages of this work were funded by the National Science Foundation through Grant DRM81-19425 to the Materials Research Laboratory at Case Western Reserve University. R.W.G. is grateful to the Department of Chemistry and Computing Center at the University of Keele for the use of their facilities and to Professor C. R. A. Catlow for informative discussions.

Aromaticity as a Quantitative Concept. 1. A Statistical Demonstration of the Orthogonality of "Classical" and "Magnetic" Aromaticity in Five- and Six-Membered Heterocycles

Alan R. Katritzky,*,‖ Piotr Barczynski,‖,‡ Giuseppe Musumarra,§ Danila Pisano,§ and Miroslaw Szafran‖,‡

Contribution from the Department of Chemistry, University of Florida, Gainesville, Florida 32611, Dipartimento di Scienze Chimiche, Università di Catania, Viale A. Doria, 8-95125 Catania, Italy, and the Department of Chemistry, A. Mickiewicz University, Poznan, Poland. *Received January 19, 1988*

Abstract: Twelve characteristics comprising readily available geometrical, energetic, and magnetic data for the nine compounds benzene, pyridine, pyrimidine, pyrazine, thiophene, furan, pyrrole, pyrazole, and imidazole are assembled and treated by principal component analysis (PCA). Three principal components (PC) are found which account for 83% of the variance of the data. Values for the characteristics of the individual compounds recalculated from the scores and loadings are in good agreement with those used in the treatment. Scores are then estimated from the limited available data for an additional seven compounds (pyridazine, *s*-triazine, 1,2,4-triazine, thiazole, oxazole, isoxazole, and 1,2,4-triazole) by fitting them into the PC model; satisfying agreement is also found between the observed and recalculated values of the characteristics. This means that the scores and loadings can be used with some confidence to predict values of characteristics not available. The first and second PC scores for the whole group of 16 compounds divide them up into the four principal chemical groups of heterocyclic aromatics: (a) pyridine (and benzene), both positive; (b) other azines, t_1 positive and t_2 negative; (c) five-member heteroaromatics with one heteroatom, t_1 negative and t_2 positive; and (d) azoles, t_1 and t_2 both negative (except oxazole which lies in group (c)). The loadings for the characteristics divide them up into three groups: in group (a) $I_{5,6}$, ΔN and (to a somewhat lesser extent) DRE, ^{15}N, and HSRE are dominated by t_1, whereas in group (b) χ_m and Λ are almost independent of t_1 but strongly dependent on t_2 and t_3. This indicates that the "classical" and "magnetic" concepts of aromaticity are almost completely orthogonal. The other characteristics show hybrid dependence.

Aromaticity is arguably the most important general concept for the understanding of organic chemistry in general and of heterocyclic chemistry in particular.[1-6] Its influence is ubiquitous in determining stability and reactivity, the nature of the reaction products to be expected, the symmetry and geometry of molecules,

‖ University of Florida.
‡ Università di Catania.
§ On leave from A. Mickiewicz University.

(1) Bergmann, E. D.; Pullman, B. Eds. *Aromaticity, Pseudo-Aromaticity, Anti-Aromaticity*; Israel Academy of Science and Humanities: Jerusalem, 1971; Jerusalem Symp. Quant. Chem. Biochem., Vol. III.

0002-7863/89/1511-0007$01.50/0